UCRL-51755

SEISMIC RESPONSE AND FAILURE ANALYSES OF A MIXED-OXIDE FUEL FABRICATION PLANT

F. J. Tokarz
R. C. Murray
H. C. Sorensen

February 14, 1975

Prepared for U.S. Energy Research & Development Administration under contract No. W-7405-Eng-48

Printed in the United States of America
Available from
National Technical Information Service
U.S. Department of Commerce
5285 Port Royal Road
Springfield, Virginia 22151
Price: Printed Copy $___*; Microfiche $2.25

*Pages	NTIS Selling Price
1-50	$4.00
51-150	$5.45
151-325	$7.60
326-500	$10.60
501-1000	$13.60

TID-4500, UC-38
Engineering and Equipment

LAWRENCE LIVERMORE LABORATORY
University of California / Livermore, California / 94550

UCRL-51755

SEISMIC RESPONSE AND FAILURE ANALYSES OF A MIXED-OXIDE FUEL FABRICATION PLANT

F. J. Tokarz
R. C. Murray
H. C. Sorensen

MS. date: February 14, 1975

Contents

SEISMIC RESPONSE AND FAILURE ANALYSES OF A MIXED-OXIDE FUEL FABRICATION PLANT

Abstract

We studied the structural integrity and possible failure modes of mixed-oxide fuel fabrication plants (MOFFP) subjected to different ground-motion intensities ranging from 0.1- to 1.0-g peak accelerations. To perform this study, we developed calculation models of safety-related systems to be used in the analysis. We performed both elastic and inelastic dynamic response analyses for both horizontal and vertical ground motion. Our conclusions regarding the structural integrity for the model MOFFP are as follows: 1) no structural damage at ground motions < 0.4 g; 2) severe structural damage at 0.4 to 0.5 g; 3) complete building collapse at >0.5 g; 4) building collapse before equipment failure.

Summary

We performed a study to evaluate the structural integrity and possible failure modes of mixed-oxide fuel fabrication plants (MOFFP) subjected to various ground-motion intensities ranging from 0.1- to 1.0-g peak ground accelerations. Because of the presence of plutonium oxide and uranium oxide at these plants, this information is needed to provide a technical basis for information included in the U. S. Nuclear Regulatory Commission assessment of the environmental impact and public risk associated with siting MOFFP's.

A significant portion of the study involved the development of calculational models of safety-related systems to be used in the analysis, with primary emphasis on the main structural systems of the manufacturing building. These safety-related systems include both glove boxes and barriers, the PuO_2 storage bins, final HEPA filter frames, ducting, and utility piping. These systems comprise the confinement system that limits a potential release of plutonium oxide.

The MOFFP used in our calculations was carefully designed to model a "representative" facility. It is expected that most future MOFFP's will be located east of the Continental Divide near reprocessing plants and power reactors. In that region, tornado rather than earthquake criteria will generally govern the external structural design while seismic criteria will influence the design of internal equipment and piping. The design earthquake ground-motion levels would be in the 0.1- to 0.2-g range.

We performed both elastic and inelastic dynamic response analyses on the main structure. Ground motion used for input was based on AEC Regulatory Guide 1.60 (Ref. 1). Damping values used were

consistent with AEC Regulatory Guide 1.61 (Ref. 2). Both horizontal and vertical response analysis were conducted, with each treated separately.

The results of our horizontal inelastic response analyses for MOFFP's founded on hard sites (shear velocity of 8000 fps) show that below 0.6-g maximum horizontal ground acceleration, the main building shows no appreciable damage (i.e., no extensive cracking). At 0.8 g and greater, the total lateral resisting capacity of the building is exceeded and the building collapses. For MOFFP's on intermediate (shear velocity of 2000 fps) or soft (shear velocity of 500 fps) sites, extrapolation from the elastic response analysis including soil-structure interaction effects shows that total building collapse from lateral motions occurs in the 0.5- to 0.6-g range of ground acceleration.

Analysis of vertical motions shows that roof slab damage occurs at about 0.4 g; the floor slab and most of the roof slab show plastic deformation at 0.5 to 0.55 g; and total collapse occurs above 0.55 g.

The conclusions regarding the structural integrity for the model MOFFP we developed are summarized below:

- No structural damage at ground motions < 0.4 g.
- Severe structural damage at 0.4 to 0.5 g.
- Complete building collapse at >0.5 g.

With minimal structural modifications, such as additional reinforcing steel in the walls, the building modeled for our study could be made capable of carrying ground motion levels exceeding 1 g.

Review of representative equipment located within the manufacturing building indicates that by proper design the equipment will have a natural frequency >30 Hz. The maximum acceleration the equipment will experience will then be the maximum floor acceleration. Input motion to the equipment is obtained by developing in-structure response spectra called floor spectra. These spectra include the effects of dynamic amplification of the ground motion by the structure.

We have generated floor spectra and maximum floor accelerations for our model building founded on a hard site. We found the maximum floor acceleration to be less than two times the maximum ground acceleration.

We have estimated the elastic strength of the equipment and found it able to survive acceleration levels greater than 1 to 2 g's. Inelastic analyses of equipment would increase these levels.

At ground acceleration levels <0.5 g, we do not expect any equipment failures. We expect complete building collapse before equipment failure.

Introduction

This is a final report of a study by the Lawrence Livermore Laboratory that was requested and funded by the U. S. Nuclear Regulatory Commission, Office of Standards Development.

Our study identifies probable failure modes in a model of a commercial-scale MOFFP that we subjected to various intensities of earthquake ground motion. The resulting failure modes will be used to estimate radiation-source terms for earthquake-induced accidents in commercial-scale MOFFP's.

Our study efforts included the following:

- Characterization of a model commercial-scale MOFFP to form the basis for the calculational models.
- Development of an acceleration time-history with a frequency content compatible with AEC Regulatory Guide 1.60.
- Performance of dynamic response analysis using ground-motion intensities ranging from Modified Mercalli VII (0.2 g) to X (≥1 g) earthquakes.
- Identification of failure modes associated with the various levels of ground-motion intensities.

The characterization of a typical MOFFP involved a significant portion of our study. Once it was characterized, we defined the ground motion to be used in our analysis and performed dynamic response analysis of the manufacturing building.

Background Information on MOFFP's

When reactor fuel elements are spent, they are sent to a fuel reprocessing plant where plutonium and uranium are recovered for re-use. The recovered plutonium and uranium oxides will be sent to mixed-oxide fuel fabrication plants (MOFFP), where they will be made into new fuel elements for light-water-cooled reactors. The fuel cycle for light-water-cooled reactors is shown in Fig. 1 (Ref. 3).

The MOFFP of the future (10 to 15 yr hence) is expected to produce approximately 1 metric ton of mixed-oxide fuel per day. This fuel will contain about 2 to 4% by weight of plutonium oxide and the remainder uranium oxide. Because plutonium presents a much greater radiological hazard than uranium, our study concentrates on earthquake-induced accidents in plutonium processes.

Future MOFFP's will contain many design and operational features to avoid criticality conditions and to influence or limit the potential release of plutonium. These include process confinement systems, control of process inventory, and building integrity. Process confinement includes glove boxes and associated exhaust systems in the powder steps of the process and the cladding after encapsulation of the sintered fuel pellets. Control of the fuel inventory includes separating the various steps in the process either by means of isolation (distance or barriers) or by employing parallel production lines to reduce the normal process inventory. In some facilities, similar processes are confined in separate areas, which provide

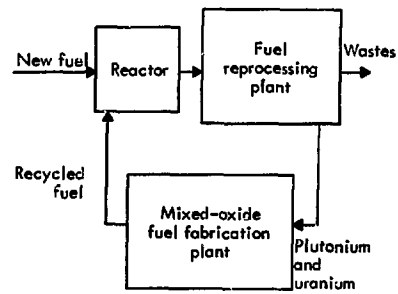

Fig. 1. Fuel cycle for light-water-cooled reactors.

additional control against release of radioactive material.

The confinement design features are usually designated as barriers. The process confinement is called the primary barrier; the separation of the processes into separate rooms is termed a secondary barrier; and the building structure and building exhaust system are generally called the final barrier. Plutonium and uranium oxides will enter the MOFFP manufacturing building in powder form. The process steps in the fabrication of fuel are shown in Fig. 2. Potential inhalation hazards exist where plutonium oxide is in powder form (steps A, B, C, D, and E). In step A, the receiving and storage area, both plutonium and uranium oxides are stored in double containers. The containers are usually in racks to prevent overturning and to provide spacing to avoid criticality accidents. Step B includes the transfer systems between various stages of the process. Either manual or mechanical transportation schemes are used to move the plutonium-oxide powder.

Weighing and blending, steps C and D, are both performed in a gloved barrier. In the remaining processes (milling, pressing, sintering, grinding, cleaning, and loading into fuel rods), the plutonium oxide is not readily dispersible. In step E, all wastes are reprocessed by a

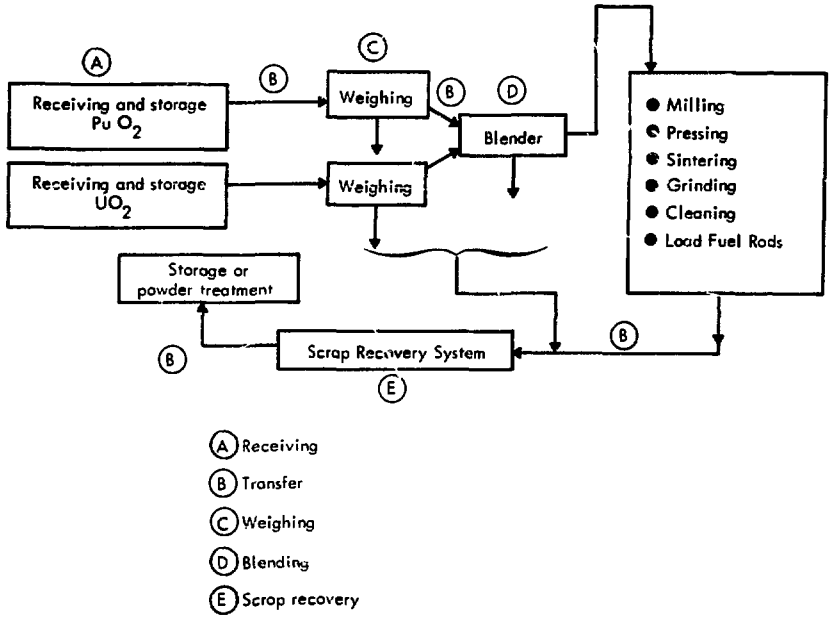

Fig. 2. Flow chart showing fuel fabrication process.

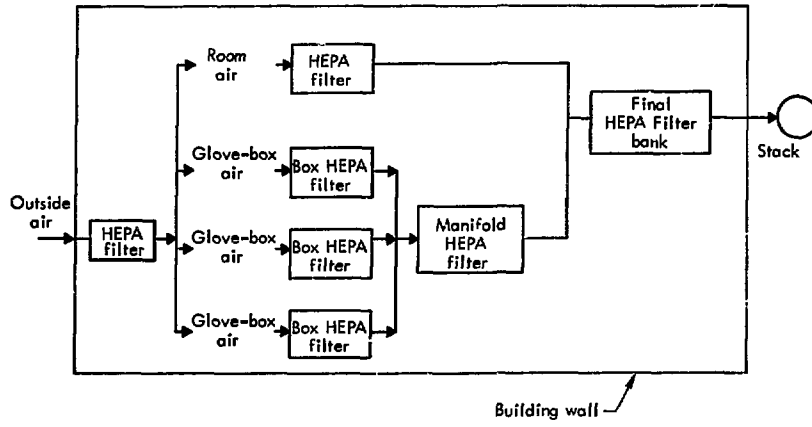

Fig. 3. Typical ventilation system.

scrap-recovery system located in glove boxes.

Figure 3 is a schematic of the ventilation system used for air cleaning in the manufacturing building. Within the manufacturing building air flow is always in the direction of greater radioactive contamination potential. The systems employ high-efficiency particulate air (HEPA) filters to minimize the release of airborne plutonium oxide from the building. Separate HEPA filters are provided for glove boxes, gloved barrier, and work rooms. Air is filtered when it enters the plant, when it enters glove boxes and gloved barriers, when it leaves the glove boxes and gloved barriers, when it leaves the work areas, and, finally, when it leaves the building through a final HEPA filter bank. The final double-HEPA filter bank is a critical part of the final confinement barrier.

Characterization of MOFFP Structures for Analysis

The model MOFFP that we characterize for our study must be reasonably representative of future MOFFP designs if we are to consider our results as representative. We used several sources of information for our design:

- A review of the License Application for the Westinghouse Recycle Fuels Plant to be located in Anderson, South Carolina.[4] This plant will have an annual receipt of material sufficient to produce approximately 200 metric tons/year initially, and approximately 400 metric tons/year in the future.
- Discussions with personnel from the Ralph M. Parsons Company who are currently designing the Westinghouse plant. The discussions dealt primarily

with alternative building layouts and equipment for future plants.

- Information obtained from a visit, and discussions at the EXXON Nuclear Plant (40 metric tons per year) in Richland, Washington. Our discussion concentrated on typical equipment that might be used
- Discussions with Battelle Northwest personnel.[5]

MANUFACTURING BUILDING STRUCTURE

Our study emphasized an evaluation of the main structure of the manufacturing building (final confinement barrier). We also examined glove boxes and gloved barriers (primary confinement barrier), a PuO_2 storage bin, the ventilation system ducting, the final HEPA filter bank (final confinement barrier), and utility piping.

General Layout

The manufacturing building of a future MOFFP is assumed to be a two-story structure. Figure 4 shows what we consider to be a representative layout of work areas in the building. The emergency power supply, waste-handling equipment, building exhaust system, and powder storage and scrap recovery areas are on the second floor. The first floor (ground level) includes the emergency control room and areas for chemical analysis, fuel fabrication, sintering furnaces, weighing, and blending. Areas where plutonium is in powder form will be enclosed by a restricted access barrier and is called the "canyon" area. The canyon area is assumed to extend from first floor to the roof.

Structural Features of Manufacturing Building

Figure 5 shows a plan and elevation that define our typical manufacturing building. The building is 210 ft square with 18-in.-thick reinforced concrete roof, floors, and walls. The first story extends 20 ft above grade, with the roof 50 ft above grade. The structure is assumed not to extend below grade.

The vertical load-carrying system consists of slabs spanning between supporting

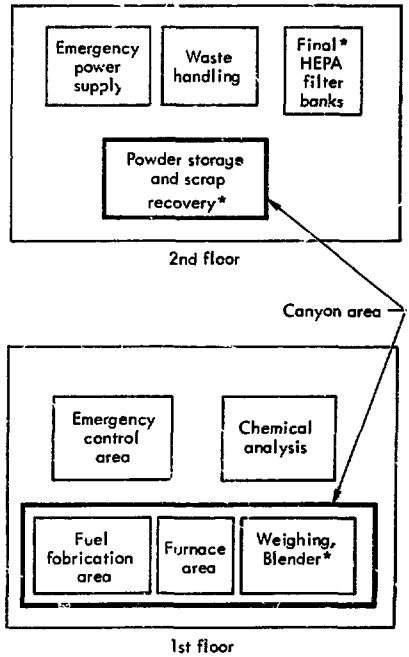

*Areas where PuO_2 can be in powder or dispersed form.

Fig. 4. Typical areas within manufacturing building.

edge beams that bear on 24 × 24 in. columns on 30 ft centers each way. At end bays, the exterior walls act as bearing walls. Should heavy equipment be located on the second floor, additional beams would be provided to carry the added load.

The lateral force-resisting system consists of floor and roof slabs and shear walls. The slabs are assumed to act as rigid concrete beams (diaphragms) spanning between exterior shear walls that are parallel to the direction of applied forces.

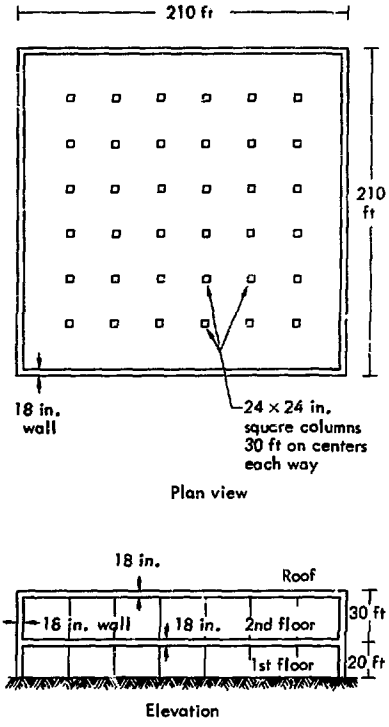

Fig. 5. Typical manufacturing building of a MOFFP.

The shear walls transmit the loads to the foundation. Adequate space between the manufacturing building and adjacent structures is assumed to accommodate differential motions.

End walls perpendicular to the direction of lateral loadings were not considered effective lateral resisting members. The interior canyon walls were treated as partition walls and were not considered part of either the vertical or lateral force-resisting systems. The interior columns were also assumed to have no lateral load-resisting capacity.

Design Basis of Manufacturing Building

Most MOFFP's (perhaps as many as 90%) expected to be built in the next 30 yr will be located east of the Continental Divide near fuel reprocessing plants and nuclear power reactors (typically near electrical load centers). This would result in typical MOFFP manufacturing building external structural designs being governed by Region I tornado criteria. Figure 6 shows the different tornado intensity regions across the country as specified for power reactors by the Directorate of Regulatory Standards. The variation in design basis characteristics is governed by the maximum wind speed and atmospheric pressure change associated with the different regions. U. S. AEC Regulatory Guide 1.76 and ANSI A58.1-1972 (Refs. 6 and 7) define the tornado design loading. Our representative manufacturing building external structural design was governed by these criteria.

Both the roof and walls are designed for 500-psf tornado loading. The roof is

considered as a slab that distributes the load in both horizontal directions, while the walls are treated as slabs that distribute the load between the floor and/or roof levels. Horizontal steel in the walls is the minimum required for shrinkage and temperature considerations. The floor and columns are designed for 400 psf floor loading (175 psf live and 225 psf dead load). The floor is considered a two-way slab and the columns as doubly-reinforced tied members. Ultimate strength design concepts[8] are employed throughout, assuming 3000 psi concrete and reinforcing steel with minimum yield strength of 40,000 psi. Figure 7 shows the reinforcing details. Design of the floors and columns will be governed by seismic criteria. An 18-in. floor slab appears to be a reasonable thickness to minimize seismic loads to equipment.

Seismic considerations played no part in arriving at our final MOFFP manufacturing building external structural design. Seismic criteria in Region I give peak-design ground motion levels in the 0.1- to 0.2-g range, so tornado design criteria are overriding. In Regions II and III, however, the tornado loading decreases by a factor of about 2 over Region I, while the seismic loads approach the 0.5- to 0.6-g level. This change in loading means that seismic criteria will usually control the external structural design in Regions II and III. MOFFP's built in these regions will be considered on a case-by-case basis.

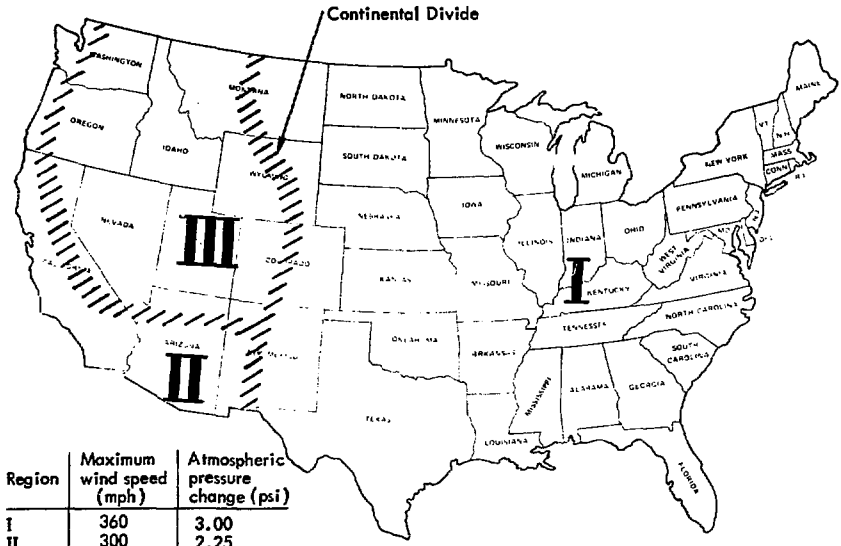

Region	Maximum wind speed (mph)	Atmospheric pressure change (psi)
I	360	3.00
II	300	2.25
III	240	1.50

Fig. 6. Tornado intensity regions. Source: U. S. AEC Regulatory Guide 1.76 (1974).

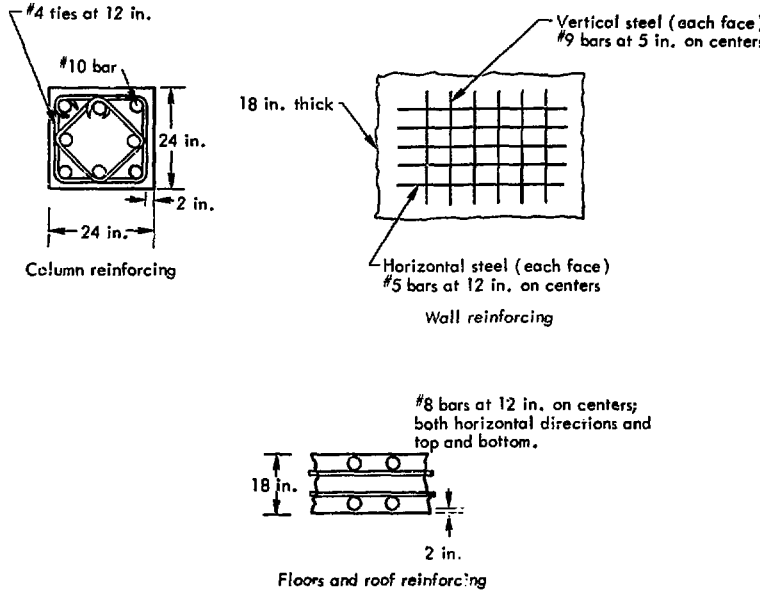

Fig. 7. Reinforcing details of walls, roofs, floor, and columns.

EQUIPMENT AND PIPING

Review of representative equipment located within the manufacturing building indicates that by proper design and location of attachments, the equipment will have a natural frequency >30 Hz. The maximum acceleration the equipment will experience will then be the maximum floor acceleration. Input motion to the equipment is obtained by developing floor spectra. These spectra include the effects of dynamic amplification of the ground motion by the structure.

We have generated floor spectra and maximum floor accelerations for our model building founded on a hard site. We found the maximum floor acceleration to be less than two times the maximum ground acceleration.

This section includes our estimates of the elastic strength of the equipment.

Glove Boxes and Gloved Barriers

All processes and operations that involve quantities of plutonium oxide in powder form sufficient to cause potential inhalation hazard are performed in glove boxes or gloved barriers. These processes include weighing, blending, milling/pellet pressing, and scrap recovery. The glove boxes are used for the process confinement of weighing and scrap recovery operations. The blending and milling/pellet pressing operations are performed in gloved barriers.

Both the glove boxes and gloved barriers are assumed located within a restricted access area. This access area is part of the canyon construction enclosing the main fabrication, powder storage, and scrap recovery areas. The canyon area is assumed to be constructed of 8-in. concrete block walls spanning between pilasters 10 ft apart. All concrete block cells are assumed filled with grout, and reinforcement is assumed in the horizontal and vertical directions.

Figure 8 shows what we considered a representative glove box design. The glove box is constructed of 12-gage stainless steel with a 3/8-in. shatter-proof glass window. It is 30×42×96 in. and weighs 5000 lb with the process equipment. The glove box is fastened to a structural steel support frame that is anchored to the floor of the main building structure.

The gloved barrier (Fig. 9) is made of 10-in. thick reinforced concrete. It extends from first floor level to the second floor and is about 5.5×8.5 ft.

Experience at LLL indicates that the glove boxes and gloved barriers can withstand floor acceleration levels greater than 1 g.

An examination of possible penetration of the stainless steel portion of the glove box because of concrete spalling or falling objects, such as piping, was conducted. Results indicate objects greater than 100 lb are needed for penetration. Objects of this size (concrete chunks) are not available prior to total collapse of the main building.

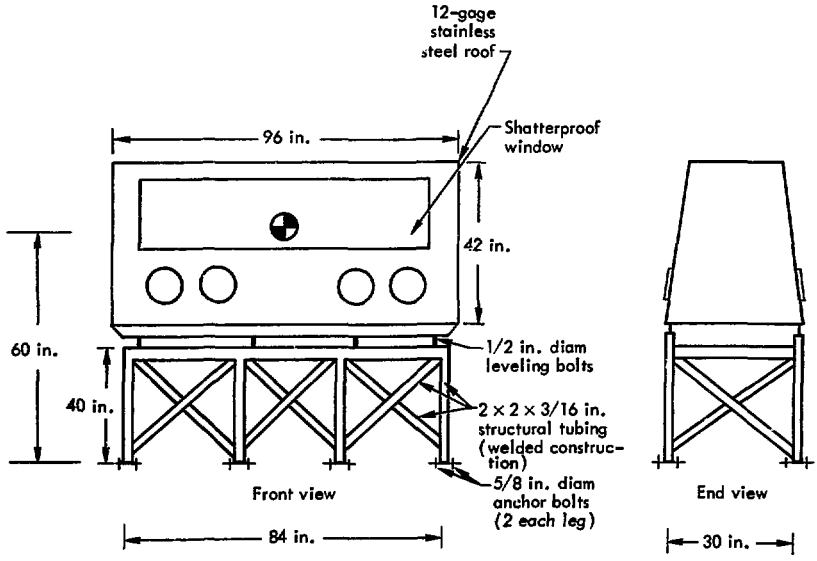

Fig. 8. Typical glove box design (weight about 5000 lb).

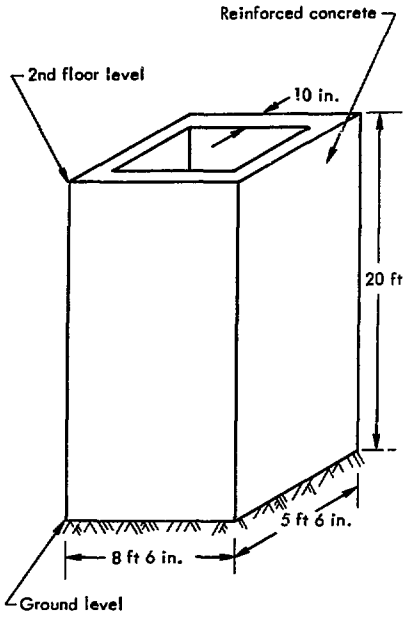

Fig. 9. Representative gloved barrier for blender.

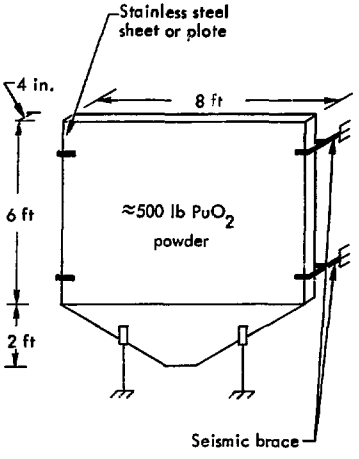

Fig. 10. Representative PuO_2 storage bin. Seismic brace will prevent lateral motion and allow vertical motion for weighing.

PuO_2 Storage Bins

PuO_2 powder is stored in bins prior to weighing and blending. These bins must be designed to receive powder from the transfer system, avoid criticality conditions, and inventory the powder by weighing. Weighing may be accomplished by picking up the bin. A representative storage bin is shown in Fig. 10. We have chosen to support the bin by two seats and have provided four braces for lateral support as shown. The weight of the bin and powder has been estimated to be 1500 lb. The integrity of the bin to seismic motions will be governed by the adequacy of the support. Estimates of support requirements indicates that braces can be designed to handle seismic loads resulting from acceleration of many g's.

Ventilation System and Utility Piping

We considered the ventilation system shown in Fig. 3 to be reasonably representative of a typical system. We restricted our examination to the final HEPA filter bank. A failure of the final HEPA filter could produce a large potential leak path.

Figure 11 shows a HEPA filter frame designed by ORNL-NSIC-65 guidelines.[9] These guidelines state (1) that the frame must be designed to carry a 2-psi shock loading across the bank without exceeding the elastic limit of the material, and (2) that the maximum member deflections must be limited to 0.1% of their length under a loading equivalent to 1.5 times

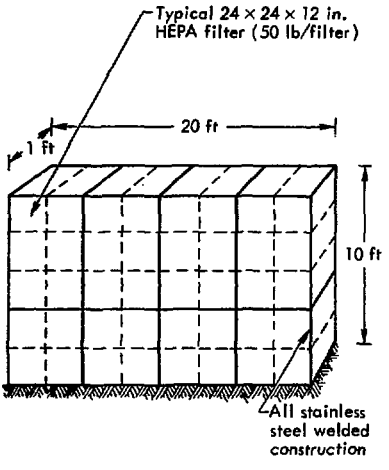

Fig. 11. Typical final HEPA filter frame.

the maximum dirty-filter pressure drop across the bank. Since these criteria are far more severe than seismic criteria, they govern the design. We judge that the structural integrity of the final HEPA filter frame is such that floor acceleration levels greater than 1 g are required to cause failures.

Because most designs do not consider the stack an effective part of the system, we also neglect it. The purpose of the stack is to start dispersion of the filtered air and provide it with an initial upward velocity. The worst type of failure expected would be a complete collapse of the stack, which would also seal the stack and prevent filtered air from leaving the building. Such a failure is very unlikely.

We did not perform an extensive structural analysis of ventilation ducting and utility piping. Both are relatively lightweight (16 gage) and are usually sufficiently anchored to the main building structure so that any failures of the ducting or piping lines would not be the result of vibratory motions. Failure would most likely result from falling objects (concrete spalling) or excessive relative displacements between anchor points that should not occur until total building collapse.

Utility lines consist of 1/2-in. diam piping containing nonexplosive mixtures of hydrogen and nitrogen, and compressed air; 1- to 3-in. diam water lines; and 3/4-in. diam hydraulic lines. Failure of any of these lines does not itself create the potential for a radioactive release. The compressed air lines could provide a means of dispersing plutonium oxide powder only if they are located in the immediate vicinity of the powder. Ventilation ducting consists of 16 gage 18-in. diam lines. A break in the ventilation ducting could be a potential source of a small radioactive release since it is anticipated that plutonium oxide would be plated on the interior walls of the ducting upstream from the final HEPA banks.

Ground Motion and Damping

We used AEC Regulatory Guide 1.60 (Ref. 1) to define the ground-motion input to our model MOFFP. Guide 1.60 describes a procedure acceptable to the NRC staff for defining response spectra for the seismic design of nuclear power plants. The guide is based on a statistical treatment of recorded ground

accelerations and response spectra of past earthquakes. It is intended for sites underlain by either rock or soil deposits, and it covers all frequencies of interest. For unusually soft sites, modification of this procedure is required.

Guide 1.60 gives both horizontal and vertical response spectra for different values of structural damping. All are normalized to a maximum horizontal ground acceleration of 1.0 g. Once the intensity of ground motion for a site is specified in terms of maximum horizontal ground acceleration, both horizontal and vertical spectra can be defined from Guide 1.60 simply by scaling.

In addition to specifying the ground motion in terms of response spectra, it

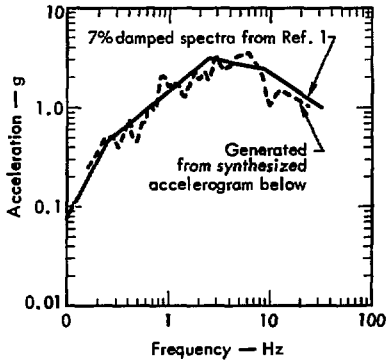

(a) Comparison of acceleration spectra

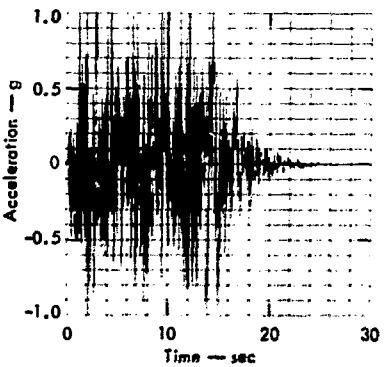

(b) Synthesized accelerogram

Fig. 12. Horizontal ground motion.

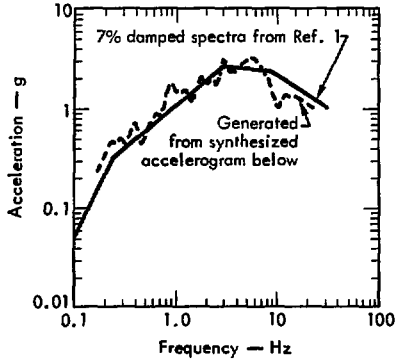

(a) Comparison of acceleration spectra

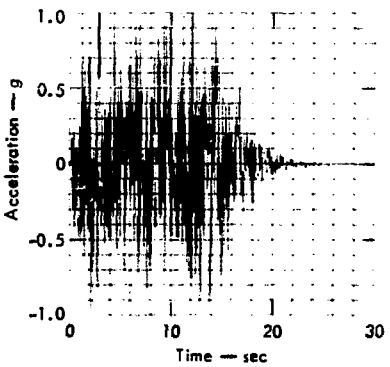

(b) Synthesized accelerogram

Fig. 13. Vertical ground motion.

was necessary to synthesize accelerograms, for input to the dynamic time-history analysis, that would reasonably reflect the frequency content of the specified spectra. We generated such accelerograms using the computer code SIMEAR.[10] In developing the accelerograms, we selected a 30-sec record with 10 to 15 sec of strong shaking. We believe that these parameters are representative of motions near large earthquakes. For examples, a magnitude 7.7 earthquake recorded at Taft, California had a duration of 30 sec and a duration of strong shaking of 10 sec. A magnitude 7.1 earthquake recorded in Olympia, Washington had duration parameters of 30 sec and 13 sec. There were no recorded data for the Charleston, South Carolina earthquake (1886), but historical accounts indicate that the near epicentral durations were within the above ranges.

Figures 12 and 13 show the horizontal and vertical response spectra and synthesized accelerograms used in this study. They are normalized to a maximum

Table 1. Modified Mercalli intensity levels.

Modified Mercalli intensity level	Approximate intensity of earthquake	Ground acceleration (a/g)
I	Detected only by sensitive instruments.	
II	Felt by a few persons at rest, especially on upper floors; delicate suspended objects may swing.	
III	Felt noticeably indoors, but not always recognized as a quake; standing autos rock slightly, vibration like passing truck.	0.005
IV	Felt indoors by many, outdoors by a few; at night some awaken; dishes, windows, doors disturbed; motor cars rock noticeably.	0.01
V	Felt by most people; some breakage of dishes; windows, and plates; disturbance of tall objects.	
VI	Felt by all; many frightened and run outdoors; falling plaster and chimneys; damage small.	0.05
VII	Everybody runs outdoors; damage to buildings varies, depending on quality of construction; noticed by drivers of autos.	0.1
VIII	Panel walls thrown out of frames; fall of wall, monuments, chimneys; sand and mud ejected; drivers of autos disturbed.	
IX	Buildings shifted off foundations, cracked, thrown out of plumb; ground cracked; underground pipes broken.	0.5
X	Most masonry and frame structures destroyed; ground cracked; rails bent; landslides.	1
XI	New structures remain standing; bridges destroyed fissures in ground; pipes broken; landslides, rails bent.	
XII	Damage total; waves seen on ground surface; lines of sight and level distorted; objects thrown up into air.	5

horizontal ground acceleration of 1.0 g. Figures 12(a) and 13(a) show the actual response spectra generated from the synthesized accelerograms, and the accelerograms are shown in Figs. 12(b) and 13(b). A comparison shows reasonable agreement over the entire frequency range of interest.

We used a 7% viscous damping value. This value is consistent with AEC Regulatory Guide 1.61 (Ref. 5), which delineates damping values acceptable for elastic dynamic analysis. The 7% value is a particularly reasonable choice for reinforced concrete structures subjected to strong ground motions. It accounts for energy dissipation and reflects both material and structural damping for stresses less than yield. Increased damping associated with stressing members beyond yield was included in our material stress-strain characterization.

Table 1 shows estimates of maximum horizontal ground acceleration corresponding to various intensity levels on the Modified Mercalli intensity scale (MM). We used this table to define different intensities of ground shaking corresponding to MM's ranging from VII (~0.2 g) to X-XII (≥1.0 g).

Analysis of the Main Structure of the Manufacturing Building

We made a seismic response analysis of the main structure of the manufacturing building. We conducted both dynamic elastic and inelastic response analyses for the horizontal and vertical directions, treating both directions separately. The elastic analysis was performed with the computer program SAPIV,[11] using the acceleration response-spectra ground motion directly. The inelastic analyses was performed with DRAIN2D,[12] using the synthetic ground-motion accelerogram developed. An equivalent viscous damping of 7% of critical was used for all calculations.

HORIZONTAL ANALYSES

Figure 14 shows the lumped mass model used to capture the horizontal response characteristics of the building. The springs K_1 and K_2 are shear springs that represent the lateral resistance of the shear walls. The mass of the building is distributed to the roof, second floor, and first floor (M_1, M_2, and M_3). The mass used at the roof level (M_1) is based on the total roof weight, one-half the second-story wall weight, and the estimated weight of the equipment attached to the wall and roof. The second-story

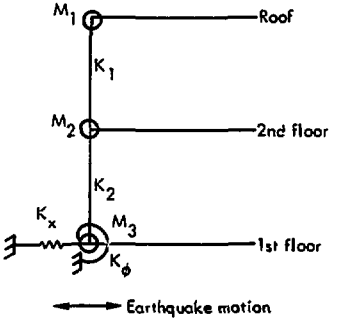

Fig. 14. Model used for horizontal response calculations.

mass (M_2) includes the weight of the floor, one-half the weight of both the first and second-story walls, and estimated equipment weight. At ground level, the mass (M_3) is based on one-half the first-story wall weights, a foundation mat, and the estimated equipment weight. Actual mass values used were 33,500, 39,000, and 24,000 lb·sec^2/in. for M_1, M_2, and M_3, respectively.

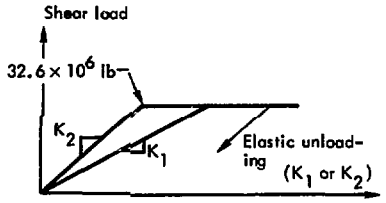

$K_1 = 300 \times 10^6$ lb/in.
$K_2 = 450 \times 10^6$ lb/in.

Fig. 15. Shear resistance of walls.

Figure 15 shows the lateral resistance characterization used. These values reflect the shear resistance of the reinforced concrete walls parallel to the direction of the motion. The lateral resistance of the columns was neglected. Elastic unloading was assumed, as was a concrete ductility ratio at 2.5.

Figure 16 defines the soil-structure spring constants used in the elastic

Site	Shear-wave velocity (ft/sec)	Soil unit weight (lb/ft^3)	Shear modulii (lb/ft^2)	K_x (lb/in.)	K_ϕ (in.-lb/rad)
Hard	8000	150	298×10^6	1.41×10^{12}	25.5×10^{15}
Intermediate	2000	125	15.5×10^6	7.33×10^8	1.33×10^{15}
Soft	500	100	0.78×10^6	3.67×10^7	6.65×10^{13}

$K_x = 2(1+\nu) G \beta_x \sqrt{BL}$

$K_\phi = \frac{G}{1-\nu} \beta_\phi BL^2$

$B = L = 210$ ft

$\nu = 0.35$

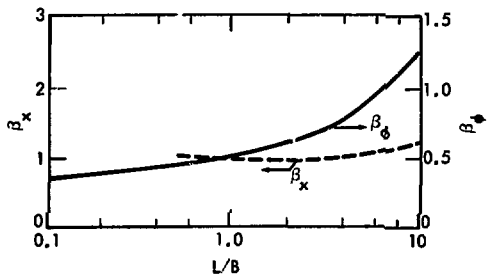

Coefficients β_x and β_ϕ for rectangular footings

G = Shear modulus of soil.

ν = Poisson's ratio of soil.

B = Foundation dimention perpendicular to applied force.

L = Foundation dimention parallel to applied force.

β_x, β_ϕ = Functions of L/B and are shown.

Fig. 16. Soil-structure interaction characteristics based on Ref. 11.

analysis (the springs are K_x and K_ϕ in Fig. 14). These values were developed from the criteria given in Ref. 13. These soil-structure interaction parameters were included because of the possibility of founding future MOFFP's on hard, intermediate, or soft sites. The soil springs reflect shear-wave velocities of 8000, 2000 and 500 fps, respectively.

Figure 17 summarizes the results of the horizontal elastic response analysis. It shows the lowest three fundamental mode shapes for each of the three sites and the corresponding fundamental periods. Values for the lowest fundamental period varied from 0.10 to 0.34 sec. The base shear and deformations are given for a 1-g peak horizontal ground-motion level.

For the inelastic analysis, the maximum lateral load capacity of each wall was determined to be 32.6×10^6 lb. This value is based on a 360-psi ultimate shear-stress capacity of the walls with web reinforcement. We assumed the horizontal

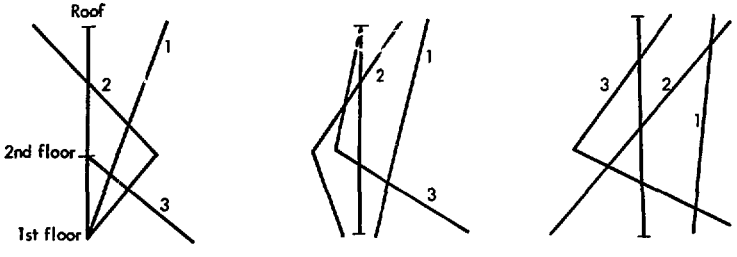

Hard site	Intermediate site	Soft site
$T_1 = 0.096$ sec	$T_1 = 0.116$ sec	$T_1 = 0.341$ sec
$T_2 = 0.047$ sec	$T_2 = 0.046$ sec	$T_2 = 0.077$ sec
$T_3 = 0.0001$ sec	$T_3 = 0.027$ sec	$T_3 = 0.034$ sec
$V_{base} = 55 \times 10^6$ lb	$V_{base} = 69.7 \times 10^6$ lb	$V_{base} = 90 \times 10^6$ lb
$\Delta_{roof} = 0.24$ in.	$\Delta_{roof} = 0.41$ in.	$\Delta_{roof} = 0.39$ in.
$\Delta_{2nd\ floor} = 0.12$ in.	$\Delta_{2nd\ floor} = 0.27$ in.	$\Delta_{2nd\ floor} = 0.35$ in.
$\Delta_{1st\ floor} = 0$ in.	$\Delta_{1st\ floor} = 0.11$ in.	$\Delta_{1st\ floor} = 0.32$ in.

1 = 1st mode
2 = 2nd mode
3 = 3rd mode

Fig. 17. Results for horizontal elastic analysis (based on spectra normalized to 1 g).

Table 2. Results from inelastic dynamic time-history analysis – (horizontal).

Acceleration level (g)	Maximum 2nd floor displacement (in.)	Maximum roof displacement (in.)	Wall shear bottom panel (psi)	Wall shear top panel (psi)
0.50	0.068	0.132	$\frac{334}{\text{yield}}$	201
0.60	0.086	0.163	360	266
0.70	0.110_1	0.189_2	360_1	284_3
0.75	0.127_1	0.206_2	360_1	292_3
0.80	$>3.0_3$	$>9.0_3$	360_3[a]	$\frac{---_3}{360_3\text{yield}}$

[a]Initial yielding occurs at 2.5 sec.

Subscript	Time of max value (sec)
1	2.5
2	4.0
3	12 - 12.5

temperature and shrinkage reinforcement also acted as web reinforcement. Neglecting the web reinforcement, yields a 190-psi ultimate value.

Table 2 summarizes the results from the horizontal inelastic-response analysis. Note that these calculations do not include soil-structure interaction effects. The building model was assumed fixed at ground level. Table 2 shows maximum floor and roof displacements and maximum shear wall stresses for different levels of ground motion. The results show that the lower shear walls exhibit inelastic deformations between 0.5- nad 0.6-g accelerations and greater. At approximately 0.75 to 0.8 g, the upper shear wall also becomes inelastic, and the total structure collapses.

VERTICAL ANALYSES

Figure 18 shows the model used to characterize the vertical load-carrying resistance of the building. It represents

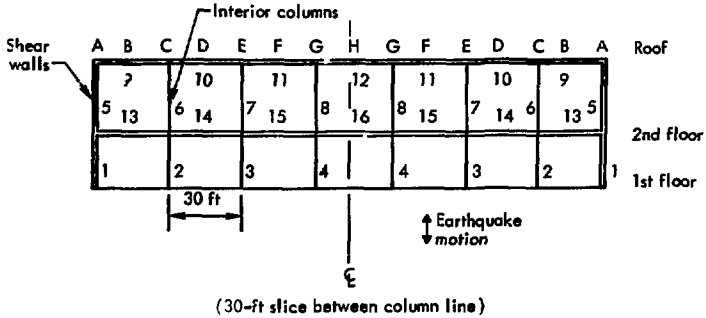

Fig. 18. Model used for vertical response calculation.

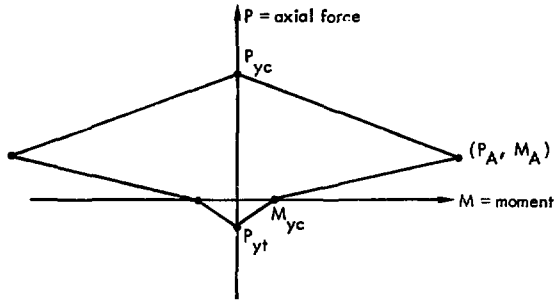

Element	P_{yc} (10^3 lb)	P_{yt} (10^3 lb)	M_{yc} (10^3 in.-lb)	P_A (10^3 lb)	M_A (10^3 in.-lb)
Wall	22,000	5,800	39,000	8,100	124,000
Columns	1,650	200	3,900	750	13,000
Roof/2nd floor	-	-	14,600	-	-

Fig. 19. Yield interaction diagram for the reinforced concrete walls, columns, roof, and walls.

the second floor and roof slabs as beams spanning between columns at interior bays and spanning to the walls at the exterior bays. The columns and walls were treated as beam-column elements.

Moments of inertia were based on gross-concrete sections. We used values of 27,700 and 175,000 $in.^4$ for the columns and floor/roof/wall sections, and cross-sectional areas of 576 and 6480 $in.^2$, respectively. Member-yield criteria were developed using ultimate-strength design concepts and a review of experimental data of failure of reinforced concrete

Table 3. Results of elastic vertical analysis.

Line[a]	Static loads		1-g earthquake	
	Max roof deflection (in.)	Max 2nd floor deflection (in.)	Max roof deflection (in.)	Max 2nd floor deflection (in.)
A	-	-	0.008	0.003
B	0.193	0.133	0.476	0.023
C	0.154	0.088	0.186	0.085
D	0.232	0.165	0.211	0.194
E	0.154	0.088	0.160	0.085
F	0.226	0.160	0.350	0.209
G	0.153	0.088	0.232	0.117
H	0.227	0.161	0.433	0.348

[a]See Fig. 18.

Table 4. Results from elastic vertical analysis – 1-g earthquake.

Roof/ 2nd floor members[a]	Max moment (10^7 in. – lb)	Max shear (10^5 lb)	Wall/ column members[a]	Max moment (10^7 in. – lb)	Max shear (10^5 lb)	Max axial force (10^5 lb)
9	2.71	2.31	1	0.36	35.6	2.47
10	1.22	2.22	2	0.12	11.6	6.18
11	1.51	1.61	3	0.06	5.85	6.09
12	1.77	1.83	4	0.22	1.39	8.42
13	0.25	0.16	5	1.44	0.55	2.41
14	0.17	0.07	6	0.16	0.07	4.83
15	1.05	1.13	7	0.10	0.05	3.76
16	1.77	1.50	8	0.13	0.05	5.56

[a]See Fig. 18.

Table 5. Results from elastic vertical analysis – static only.

Roof/ 2nd floor members[a]	Max moment (10^7 in. – lb)	Max shear (10^5 lb)	Wall/ column members[a]	Max moment (10^7 in. – lb)	Max shear (10^5 lb)	Max axial force (10^5 lb)
9	0.82	1.63	1	0.33	0.21	3.12
10	0.88	1.59	2	–	–	6.33
11	0.87	1.58	3	–	–	6.32
12	0.86	1.58	4	–	–	1.53
13	0.83	1.59	5	0.66	0.32	3.19
14	0.88	1.59	6	–	–	3.18
15	0.88	1.59	7	–	–	3.16
16	0.86	1.59	8	–	–	–

[a]See Fig. 18.

Table 6. Results inelastic vertical analysis.

Column line[a]	0.40 g + static load		0.50 g + static load		0.55 g + static load		0.57 g + static load	
	Max roof defl. (in.)	Max 2nd floor defl. (in.)	Max roof defl. (in.)	Max 2nd floor defl. (in.)	Max roof defl. (in.)	Max 2nd floor defl. (in.)	Max roof defl. (in.)	Max 2nd floor defl. (in.)
A	0.011_2	0.006_2	0.012	0.007_2	0.012_2	0.007_2	0.010_2	0.006_2
B	0.326_2	0.203_3	0.385_2	0.219_2	0.411_2	0.227_2	0.326^b_2	0.200_2
C	0.239_1	0.133_1	0.260_1	0.145_1	0.270_1	0.150_1	0.215_2	0.124_2
D	0.371_1	0.276_1	0.420_3	0.304_1	0.447_3	0.325_1	0.305^b_2	0.215_2
E	0.247_1	0.140_1	0.271_1	0.152_1	0.280_1	0.158_1	0.179_2	0.105_2
F	0.379_4	0.258_1	0.437_3	0.283_1	0.468_3	0.298_1	0.295^b_2	0.233
G	0.249_1	0.136_1	0.272_1	0.148_1	0.288_1	0.156_1	0.168_2	0.101_2
H	0.398_2	0.251	0.469_3	0.288_2	0.535_3	0.291_2	0.283^b_2	0.198_2

[a]See Fig. 18.

[b]At 10 sec, these deflections are greater than 10 in.

Subscript	Time of max deflection (sec)
1	5.02
2	8.71 - 9.32
3	12.12
4	14.39

members. Figure 19 is the yield interaction diagram used for the different structural elements. Assumed reinforcement details are shown in Fig. 7.

The mass of the building was distributed uniformly at the roof and floor levels. We used values consistent with a 30-ft slice of the building, assuming a 125-psf live load and a 225-psf dead load. The live load is typical of heavy manufacturing facilities.

Tables 3 through 5 summarize the results from the vertical elastic response analysis. Table 3 gives the maximum roof and floor level deflections resulting from static (live and dead) loads and a 1-g vertical earthquake ground motion. Tables 4 and 5 give the maximum member forces for the same two loading conditions. The first five periods of vibration were calculated as 0.129, 0.120, 0.117, 0.111, and 0.107 sec.

Table 6 and Fig. 20 summarize the results from the inelastic vertical response analysis. Table 6 gives the maximum roof and second-floor level deflections for increasing levels of earthquake ground motion varying from 0.4 to 0.57 g. Figure 20 shows pictorially the location of plastic hinge formations. Both Table 6 and Fig. 20 also show the time of occurrence of the maximum values.

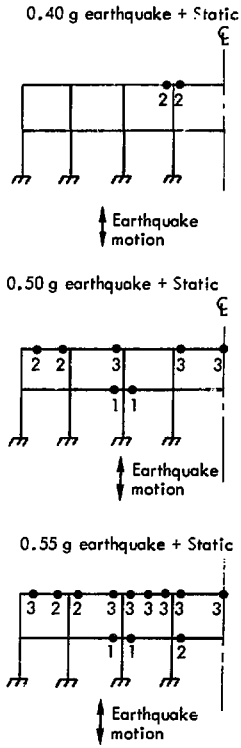

Symbol	Time of max plastic hinge formation (sec)
1	5.02
2	8.95 - 9.33
3	14.5 - 14.8

Fig. 20. Results of inelastic vertical analysis.

Results and Discussion

HORIZONTAL RESPONSE RESULTS

The inelastic horizontal-response calculation indicated no inelastic behavior or yielding for horizontal ground-motion levels below 0.5-g maximum acceleration. For ground-motion levels of 0.6 to 0.75 g, response excursions into the inelastic

range occur at the bottom shear-wall panel (ground level to second floor level). For ground-motion level greater than 0.8 g, both the bottom and top shear-wall panels have sufficient excursions into the inelastic regime to cause large displacements that lead to total collapse of the structure.

Initial yielding (i.e., shear stresses greater than 360 psi) always occurred early (at about 2.5 sec). For ground motion of 0.6 to 0.75 g, the maximum roof displacement followed at about 4.0 sec. At 0.8 g and greater, deflection of 3 in. and more were calculated at 12 to 12.5 sec.

The most valuable result we obtained from the elastic horizontal-response calculations was the establishment of trends in response variations as a function of possible soil-structure interaction effects. The soil springs used reflect site characteristics that are reasonably representative of hard, intermediate, and soft sites. The results indicate considerable variation in response characteristics for these different sites.

1) The fundamental period varied more than 300% going from the hard site to the soft (0.10 to 0.34 sec).

2) Mode shapes also showed considerable differences.

3) Both intermediate and soft site analysis results indicated considerable rigid body translation.

4) The total roof displacement for both the intermediate and soft site cases was the same and was 66% greater than in hard site cases.

5) Relative displacement for the soft site calculations was only 30% of that for the hard site. The intermediate case showed 25% greater relative displacement than the hard site.

6) Base shears increased 65% from the hard to soft site cases. This increase results from better coupling between the structural system with the ground motion.

Our elastic analysis with soil-structure interaction suggest that an inelastic analysis with soil-structure characterization would show total collapse of the building at a lower level of ground motion intensity. We feel that a reasonable estimate for total collapse of the building with soil-structure interaction effects included is in the 0.5- to 0.6-g range.

VERTICAL RESPONSE RESULTS

The elastic response analysis of the building indicates that the first five periods of vibration are very close (0.129 to 0.107 sec). Maximum roof and second floor deflections for a 1-g earthquake with static dead and live loads included are 0.23 and 0.16 in., respectively. For a 0.4-g vertical ground motion, values are 0.19 and 0.14 in.

Table 6 and Fig. 20 summarize the results from the vertical analysis. Below 0.4-g ground-motion levels, no yielding occurs. At the 0.4-g ground-motion level, yielding or plastic hinges are formed only at the innermost column line in the roof slab. At 0.5 g, most of the roof slab has yielded, as well as some at the second floor level. At the 0.55-g level, yielding is even more extensive. Above 0.55 g, the extent of yielding is sufficient to lead to a total collapse of the structure. At the 0.57-g level, most of the plastic hinges occur at 5 sec; at 10- to 11-sec deflections at the midspan of both the roof and second floor slabs all exceed 10 in.

DISCUSSION

Results indicate that below 0.6-g maximum horizontal ground motion, the main building will show no appreciable damage. At 0.8 g and greater, the total lateral resisting capacity of the building will be exceeded and the building will collapse. These conclusions are based on the inelastic response analysis, which neglects possible soil-structure effects.

If the MOFFP should be founded on intermediate or soft sites, an extrapolation from the elastic response analysis (which did account for soil-structure interaction) shows that total building collapse from lateral motions would occur in the 0.5- to 0.6-g range.

For vertical motions, results indicate that roof slab damage (e.g., concrete cracking, and spalling) will occur at approximately 0.4-g maximum ground acceleration. At 0.5- to 0.55-g levels, the floor slab and most of the roof slab exhibit plastic deformation. At ground-motion levels greater than 0.55 g, vertical motion will cause total collapse of the building.

Our examination of the primary confinement barriers in the building (glove boxes, gloved barriers, PuO_2 storage bins, and ventilation system) showed that they appear to have structural integrity to resist vibratory motions with peak floor accelerations greater than 1 g. We would anticipate failures of the ventilation ducting and utility piping only in conjunction with major failure of the main manufacturing building structure.

It is important to remember that the response characteristics of the majority of most future MOFFP's will reflect designs primarily influenced by tornado criteria, as did our own MOFFP characterization. Such a design will have response characteristics consistent with stiff brittle structures having little reserve energy capacity. These structures typically will have to meet seismic criteria of 0.1 to 0.2 g. With minimum structural modification (e.g., additional reinforcing steel in walls and slabs and perhaps closer column spacing), the building could be made capable of carrying ground motion levels exceeding the 1-g intensity level.

Acknowledgments

The authors acknowledge the assistance and encouragement of V. N. Karpenko, Leader; and C. E. Walter, Deputy Leader; Nuclear Test Engineering Division, Mechanical Engineering Department, Lawrence Livermore Laboratory.

We would like to particularly thank Dr. R. L. Gotchy, U. S. NRC, Office of Standards Development, for providing guidance and support throughout this study. His comments and suggestions have been most helpful.

We also appreciate the time spent by Mr. Kevin Barry and his associates at the Ralph M. Parsons Company, Dr. Roy Nilson of the Exxon Nuclear Company, and Lyle Schwendiman and his associates of Battelle Northwest for their aid in defining model MOFFP's.

References

1. U.S. AEC Regulatory Guide 1.60, "Design Response Spectra for Nuclear Power Plants," Rev. 1 (December 1973).
2. U.S. AEC Regulatory Guide 1.61, "Damping Values for Seismic Design of Nuclear Power Plants" (October 1973).
3. The Safety of Nuclear Power Reactors and Related Facilities, U.S. AEC Rept. WASH-1250 (July 1973).
4. License Application, Recycle Fuels Plant, Westinghouse Nuclear Fuel Division, Pittsburgh, PA (July, 1973).
5. J.M. Selby, et al., Considerations in the Assessment of the Consequences of Effluents from Mixed Oxide Fuel Fabrication Plants, Battelle Pacific Northwest Laboratories, Rept. BNWL-1697, UC41 (June 1973).
6. U.S. AEC Regulatory Guide 1.76, "Design Basis Tornado for Nuclear Power Plants" (April 1974).
7. ANSI A58.1-1972, "Building Code Requirements for Minimum Design Loads in Buildings and Other Structures," American National Standards Institute, Inc.
8. Building Code Requiements for Reinforced Concrete, Amrican Concrete Institute, Pub. 318-71 (1971).
9. C.A. Burchsted and A.B. Fuller, Design, Construction, and Testing High-Efficiency Air Filtration Systems for Nuclear Applications, ORNL-NSIC-65 (1970).
10. M. Watabe, "SIMEAR Generation of Simulated Earthquake," National Information Service; – Earthquake Engineering University of California, Berkeley, Document No. 09-573 (December 1972).
11. K.J. Bathe, E.L. Wilson and F.E. Peterson, SAPIV Structure Analysis Program for Static and Dynamic Response of Linear Systems, Earthquake Engineering Research Center, University of California, Berkeley, Rept. EERC 73-11 (1973).
12. A. Kanaan and G.H. Powell, General Purpose Computer Program for Inelastic Dynamic Response of Plane Structures, Earthquake Engineering Research Center, University of California, Berkeley, Rept. EERC 73-6 (1973).
13. R.V. Whitman and F.E. Richart, Jr., "Design Procedures for Dynamically Loaded Foundations," Soil Mechanics and Foundations Division (Nov. 1967), p. 169-193.

RAC/md/lmc